

LETTERS

Hidden Breakdown of Linear Response: Projections of Molecular Motions in Nonequilibrium Simulations of Solvation Dynamics**Michael J. Bedard-Hearn, Ross E. Larsen, and Benjamin J. Schwartz****Department of Chemistry and Biochemistry, University of California, Los Angeles,
607 Charles E. Young Drive East, Los Angeles, California 90095-1569**Received: February 13, 2003; In Final Form: April 23, 2003*

The linear response (LR) approximation forms the cornerstone of nonequilibrium statistical mechanics and has found special utility in studies of solvation dynamics, in which LR implies that nonequilibrium relaxation dynamics is governed by the same molecular motions responsible for fluctuations at equilibrium. When the motions at and away from equilibrium fall in the LR regime, the equilibrium and nonequilibrium response functions are identical. However, similarity of the equilibrium and nonequilibrium solvent response functions does not guarantee that LR holds and that the underlying molecular motions are the same. In this paper, we present computer simulation studies of the removal of charge from an atomic solute in liquid tetrahydrofuran, a system for which the equilibrium and nonequilibrium solvation responses appear quite similar. We then introduce a method for projecting nonequilibrium response functions onto specific molecular motions. We find that the equilibrium relaxation is dominated by solvent rotations, whereas the nonequilibrium relaxation is much more complex, having translations dominating at early times and a delayed onset of rotations. The results imply that LR may not hold as often as is widely believed and that care should be taken when using equilibrium response functions to understand nonequilibrium solvation dynamics.

Solvents are not just spectators during chemical reactions, nor are they simply a continuum in which a reaction occurs. Rather, the specific motions of individual solvent molecules directly affect the rate of electron transfer and other solution-phase chemical reactions. The study of how solvent motions couple to electronic changes in reacting solutes is known as solvation dynamics,¹ which is typically monitored via the solvation energy gap, $\Delta E = E_{ss}^{\text{exc}} - E_{ss}^{\text{gnd}}$, where E_{ss}^{exc} and E_{ss}^{gnd} are the solute–solvent interaction energies when the solute is in the excited and ground states, respectively. The normalized nonequilibrium solvent response function is

$$S(t) = \frac{\overline{\Delta E(\mathbf{R};t)} - \overline{\Delta E(\mathbf{R};\infty)}}{\overline{\Delta E(\mathbf{R};0)} - \overline{\Delta E(\mathbf{R};\infty)}} \quad (1)$$

where \mathbf{R} denotes all of the solute and solvent positions and the

overbar represents a nonequilibrium ensemble average in which the solute is promoted to the excited state at $t = 0$.

One of the central themes in the study of solvation dynamics is the idea of linear response (LR), which is based on the Onsager regression hypothesis.² In LR, the motions of the solute and solvent molecules that respond to a small perturbation are the same as those that follow naturally from a fluctuation away from equilibrium. In this limit, $S(t)$ is identical to the equilibrium solvation time correlation function (TCF),²

$$C(t) = \frac{\langle \delta \Delta E(0) \delta \Delta E(t) \rangle}{\langle (\delta \Delta E)^2 \rangle} \quad (2)$$

where the angled brackets denote an equilibrium ensemble average and $\delta \Delta E = \Delta E - \langle \Delta E \rangle$ is the equilibrium fluctuation of the energy gap (and the \mathbf{R} dependence is repressed). The nature of LR has been explored in simulations of myriad solute–solvent systems, and most have found that, even for very large

* To whom correspondence should be addressed. E-mail: schwartz@chem.ucla.edu. Fax: (310) 206-4038. Voice: (310) 206-4113.

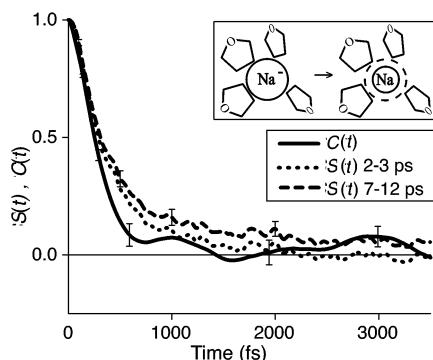


Figure 1. Comparison of the equilibrium solvation TCF, $C(t)$ (solid curve, eq 2), with the nonequilibrium solvation response function, $S(t)$ (eq 1). $S(t)$ is shown using two different values of the equilibrium energy gap, $\Delta E(\infty)$, one averaged from 7 to 12 ps after excitation (dashed curve) and the other from 2 to 3 ps after excitation (dotted curve).¹⁰ Error bars are two standard deviations.⁹ The inset shows a schematic of the reaction studied; the ground state (anion) is instantly changed into the smaller excited state (neutral) without changing the velocities or positions of the solute and THF solvent molecules.

perturbations, $S(t)$ agrees fairly well with $C(t)$.³ There have been a few notable exceptions, including simulations of a solute in methanol that undergoes a dipole reversal in the excited state,⁴ simulations in water/methanol⁵ and water/DMSO^{5,6} mixtures, and simulations in water of an atomic solute that changes both size and charge in the excited state.⁷ Despite these exceptions, LR is widely believed to hold, and many studies have elected to save computational resources by calculating only the equilibrium solvation TCF via eq 2 instead of computing $S(t)$ from an ensemble of nonequilibrium trajectories, as in eq 1.⁸

Figure 1 shows an example of both $C(t)$ (solid curve)⁹ and $S(t)$ (dashed curves) calculated from simulations modeling the removal of charge from an atomic anion in liquid tetrahydrofuran (THF), as depicted schematically in the inset to Figure 1; in addition to the removal of charge, the solute undergoes a significant decrease in size upon ionization, as described in detail in the Appendix. $S(t)$ is shown normalized with two different choices of $\Delta E(\infty)$.¹⁰ The similarity of the two response functions in Figure 1 could lead one to believe LR applies to this system.¹¹ In a previous publication, however, we have shown that in systems where the solute underwent even small changes in size, linear response failed to properly describe the nonequilibrium solvation dynamics.⁷ Thus, we were surprised to see the apparent agreement between $C(t)$ and $S(t)$ in Figure 1, in which the solute size decrease was chosen to mimic a physically realistic system (see Appendix). In this letter, we show that the similarity between the equilibrium and nonequilibrium solvent response functions in Figure 1 is coincidental and that LR fails for this system. This result has important implications for studies of solvation dynamics because it establishes that the nonequilibrium solute–solvent motions underlying relaxation can be different from those at equilibrium, even when similar relaxation time scales suggest otherwise. To demonstrate how the nonequilibrium solvation dynamics differ from those at equilibrium, we will project the relaxation dynamics inherent in both $S(t)$ and $C(t)$ onto the dynamics of various coordinates of the system.

Perhaps the simplest possible projection is to split the solute–solvent interaction, which consists of Coulomb plus Lennard-Jones potentials (as described in the Appendix), into its component parts. Such a partitioning of the solute–solvent energy gap into simple components is hardly novel; Berkowitz and Perera, for example, showed how the nonequilibrium ΔE is modulated by different solvent shells.¹² We choose to write the solvation

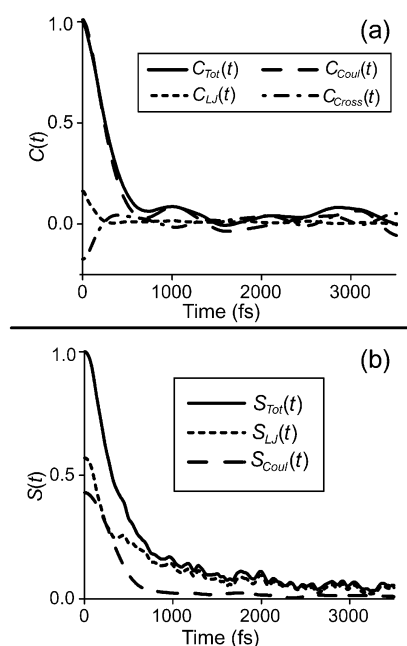


Figure 2. Solvation energy projections for (a) the equilibrium dynamics and (b) the nonequilibrium simulations: Coulomb (dashed curves), Lennard-Jones (dotted curves), and total (solid curves, same data as in Figure 1). The cross term (dash-dot curve) is from the correlation of the Coulomb and Lennard-Jones energy gaps.¹⁰

energy gap as a sum of Coulomb plus Lennard-Jones gaps, $\Delta E = \Delta E_{\text{Coul}} + \Delta E_{\text{LJ}}$. Inserting this separation into eqs 1 and 2 allows us to discern how the Lennard-Jones and Coulomb interactions contribute separately to the behavior of the equilibrium TCF, $C(t)$, and the nonequilibrium response function, $S(t)$.

Figure 2 shows the projection onto the Coulomb (dashed curves) and Lennard-Jones (dotted curves) components of the equilibrium solvation TCF and nonequilibrium solvation energy gap for the simulations of which the full response functions are shown in Figure 1. The projections in Figure 2 clearly demonstrate a hidden breakdown of LR: the relaxation dynamics underlying $C(t)$ is mostly electrostatic in nature, but the dynamics of $S(t)$ is nearly evenly distributed between charge (Coulomb) and size (Lennard-Jones) interactions, each of which relaxes at a different rate. Figure 2a also displays a nontrivial, negative cross-term for the equilibrium TCF (dash-dot curve), whereas no such energy cross-term is possible in the nonequilibrium analogue, $S(t)$.

Although the energy projections in Figure 2 reveal a breakdown of LR, they do not provide information about the specific molecular motions present at equilibrium and during nonequilibrium solvation dynamics (e.g., how modulation of the Lennard-Jones interaction may result from molecular translations or rotations). To see just which motions cause the equilibrium relaxation, we will use Steele theory,¹³ which shows how to analyze the degrees of freedom underlying any time correlation function by investigating its second time derivative; for example, the equilibrium solvation velocity TCF is given by

$$G(t) = -\ddot{C}(t) = \langle \Delta \dot{E}(t) \cdot \Delta \dot{E}(0) \rangle \quad (3)$$

The chain rule for differentiation is applied to write the rate of change of the energy gap as a sum of contributions from each degree of freedom present in the system

$$\Delta \dot{E} = \sum_{\alpha} \frac{d\alpha}{dt} \frac{\partial \Delta E}{\partial \alpha} = \sum_{\alpha} \Delta \dot{E}_{\alpha} \quad (4)$$

where the sum on α runs over all degrees of freedom. By inserting eq 4 into eq 3, we project $G(t)$ onto each of the molecular motions via the velocities, $d\alpha/dt$, and thus, $G(t)$ may be written as a sum of correlation functions of the individual degrees of freedom plus cross-correlation terms. Ladanyi and co-workers have used $G(t)$ to show how molecular rotations, translations, and rotation/translation coupling drive equilibrium solvation dynamics in both polar and nondipolar solvents.^{3c,14,15} Similar projections also have been used to analyze the force autocorrelation function, which determines vibrational relaxation.¹⁵

Here, we extend Steele theory to nonequilibrium solvation dynamics to uncover the reasons for the breakdown of LR evident in Figures 1 and 2. By decomposing the unnormalized Stokes shift into its single-molecule components, $\Delta E(t) = \sum_{i=1}^{\text{nmol}} \Delta E_i(t)$ and taking the first time derivative, we obtain the single-molecule velocity nonequilibrium response function, $J_i(t)$,

$$J_i(t) = \Delta \dot{E}_i(t) = \sum_{\mu} \Delta \dot{u}_{\mu}(r_{\mu 0}; t) = \sum_{\mu} [\dot{\mathbf{r}}_{\mu} \cdot \hat{\mathbf{r}}_{\mu 0} - \dot{\mathbf{r}}_0 \cdot \hat{\mathbf{r}}_{\mu 0}] \Delta u_{\mu}'(r_{\mu 0}) \quad (5)$$

where the sum over μ runs over the sites on the i th solvent molecule and we have defined $\Delta E_i(\mathbf{R}_i; t) = \sum_{\mu=1}^{\text{sites}} \Delta u_{\mu}(r_{\mu 0}; t)$, where $r_{\mu 0}$ is the distance from the μ th site to the solute, $u_{\mu}(r)$ represents a pairwise site-site interaction, $\Delta u_{\mu}(r)$ is the difference between the ground- and excited-state pair interactions, $\hat{\mathbf{r}}_{\mu 0}$ is $\mathbf{r}_{\mu 0}/r_{\mu 0}$, and $\Delta u_{\mu}'(r_{\mu 0}) = (d/dr_{\mu 0})\Delta u_{\mu}(r_{\mu 0})$. We account for all degrees of freedom in eq 5 by explicitly including both solute and solvent velocities.

Although eq 5 projects changes in the energy gap onto molecular velocities, taking only one time derivative does not extract information about cross-terms between the different molecular motions. Thus, we take the second time derivative of $\Delta E_i(t)$ to make the closest nonequilibrium analogy to $G(t)$, eq 3. We define the solvation acceleration response function, $B_i(t)$, as

$$-B_i(t) = \Delta \ddot{E}_i(t) = \frac{d}{dt} J_i(t) = \frac{d}{dt} \left[\sum_{\mu} \dot{\mathbf{r}}_{\mu 0} \cdot \hat{\mathbf{r}}_{\mu 0} \Delta u_{\mu}'(r_{\mu 0}) \right] = \sum_{\mu} [\dot{\mathbf{r}}_{\mu 0} \Delta u_{\mu}'(r_{\mu 0})] \cdot \dot{\mathbf{r}}_{\mu 0} + \sum_{\mu} \left[\frac{\Delta u_{\mu}''(r_{\mu 0})}{r_{\mu 0}} \right] \times |\dot{\mathbf{r}}_{\mu 0}|^2 - \sum_{\mu} \dot{\mathbf{r}}_{\mu 0} \cdot \left[\dot{\mathbf{r}}_{\mu 0} \left(\frac{\Delta u_{\mu}'(r_{\mu 0})}{r_{\mu 0}} - \Delta u_{\mu}''(r_{\mu 0}) \right) \hat{\mathbf{r}}_{\mu 0} \right] \cdot \dot{\mathbf{r}}_{\mu 0} \quad (6)$$

where we have simplified the notation by introducing $\dot{\mathbf{r}}_{\mu 0} = \dot{\mathbf{r}}_{\mu} - \dot{\mathbf{r}}_0$, and $\hat{\mathbf{r}}_{\mu 0} = \mathbf{r}_{\mu} - \mathbf{r}_0$. Equation 6 shows how changes in the energy gap are projected onto both molecular velocities and accelerations; the last term in square brackets in eq 6 is a dyadic matrix that explicitly contains cross-coordinate terms. Neither the projections onto accelerations nor the cross-coordinate terms are features present in the equilibrium analysis based on eq 3 (because the cross terms in $G(t)$ come from the nature of the correlation function and not directly from the derivatives). We have found that the acceleration term dominates in eq 6.

As written, each component of eq 6 projects the solvation energy gap onto the individual atomic coordinates in the simulation. We, however, wish to examine the relative molecular motions (e.g., translations or rotations) between the solute and solvent molecules that affect the energy gap. In the case of

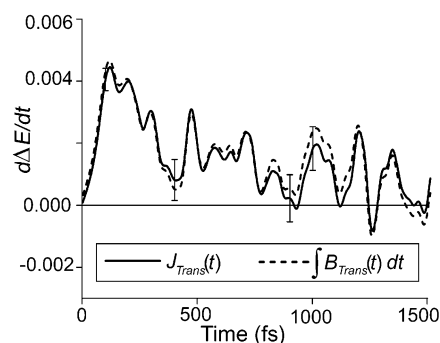


Figure 3. Comparison of $\Delta \dot{E}_{\text{trans}}(t)$, calculated both analytically as $J_{\text{trans}}(t)$ (solid curve, eq 5) and as one time integral of $B_{\text{trans}}(t)$ (dashed curve, integral of eq 6), showing that the nonequilibrium rotation/translation cross term is negligible. Error bars are one standard deviation.

relative translations between the solute and solvent center-of-mass, $B_{\text{trans}}(t)$, for example, there is one longitudinal translation along the line connecting each solvent molecule's center of mass to the solute and two indistinguishable (and arbitrary) lateral translations perpendicular to the longitudinal direction.¹⁶ Thus, armed with eqs 3 and 6, we can directly compare the projections of different solute and solvent motions onto the energy gap at equilibrium and during nonequilibrium dynamics.

Although projections onto molecular motions result in derivatives of solvation response functions, differentiated functions such as $G(t)$ or $B(t)$ do not provide an intuitive means for visualizing solvation dynamics. For example, a projected solvation velocity TCF provides information only about the curvature and not about the underlying relaxation time scales of the projected motions to the full response. Furthermore, upon differentiation, information about the relative magnitude of the projected energy change is lost. The magnitude information is important because it quantifies how strongly a particular degree of freedom contributes to the full solvation response function. Therefore, we analyze our response functions by doubly time integrating the projected $G(t)$ and either doubly integrating the projected $B(t)$ or singly integrating the projected $J(t)$.

Unfortunately, the 200 nonequilibrium trajectories that we ran for our system did not provide sufficient convergence for accurate double integration of $B_{\text{trans}}(t)$. Thus, in Figure 3, we compare the single time integration of the center of mass translational projection from $B(t)$ (dashed curve) to the center-of-mass translational projection of $J(t)$ (solid curve). We expect the two curves not to be identical because the velocity projection $J_{\text{trans}}(t)$ implicitly contains rotation/translation cross terms, while the integral of $B_{\text{trans}}(t)$ does not. Nevertheless, it is clear from Figure 3 that for this system (especially at early times when LR appears to hold)¹¹ the rotation/translation cross terms are negligible. Therefore, $S_{\text{trans}}(t)$, the projection of $S(t)$ onto the center-of-mass translational coordinate, can be accurately calculated by a single time integral of $J_{\text{trans}}(t)$ with much less numerical error than by double integration of $B_{\text{trans}}(t)$.

Figure 4a shows the doubly integrated projections of the equilibrium solvation velocity response, $G(t)$, normalized to the total, while Figure 4b shows a similar comparison for the singly integrated projections of the nonequilibrium solvation velocity response, $J(t)$. The rotational projections (dashed curves) were calculated by subtracting the translational projection (dotted curves) from the total (solid curves), so that $C_{\text{rot}}(t)$ in Figure 4a also includes rotation/translation cross terms. Even at the earliest times, it is clear that the fundamental solvation dynamics responsible for relaxation are entirely different. Thus, Figures 2 and 4 show that there is a hidden breakdown of linear response

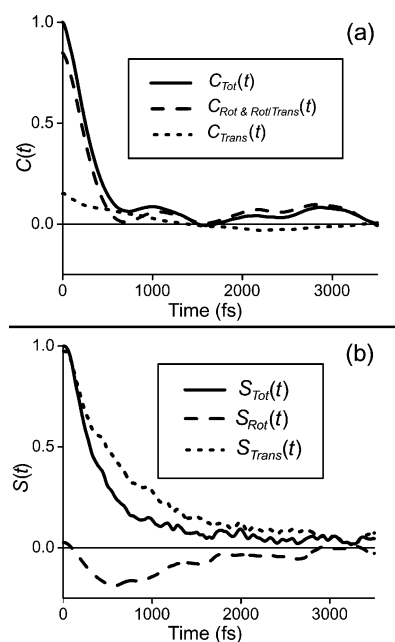


Figure 4. Translational projection of (a) the equilibrium solvation TCF, $C(t)$, shown as two time integrals of the projected $G_{\text{trans}}(t)$ (dotted curve, eq 3). The rotation and rotation/translation term (dashed curve) is calculated by subtracting $C_{\text{trans}}(t)$ from $C_{\text{tot}}(t)$ (solid line, same as solid curve in Figure 1); see text. Panel b shows similar projections of the nonequilibrium solvation response function, $S(t)$, shown as one time integral of $J_{\text{trans}}(t)$ (dotted curve). $S_{\text{rot}}(t)$ (dashed curve) is calculated by subtracting $S_{\text{trans}}(t)$ from $S_{\text{tot}}(t)$ (solid curve, same as dashed curve in Figure 1).¹⁰

in this system and that, as expected on the basis of our previous study,⁷ linear response does fail when solutes undergo significant changes in size upon excitation.

Figures 2a and 4a show that the equilibrium TCF, $C(t)$, is dominated by rotations and Coulomb-like interactions at all times. In contrast, Figures 2b and 4b show that the nonequilibrium solvation response appears to have three different relaxation regimes. Immediately upon excitation, Figure 4b shows that the primary relaxation dynamics come from translations. This is because the decreased size of the neutral excited state creates space near the solute. Solvent molecules near the solute translate into this space and fall into the Lennard-Jones well, thereby stabilizing the neutral solute and greatly destabilizing the anionic ground state. Figure 4b also shows that the second relaxation regime, from ~ 400 to 1500 fs, is characterized by the onset of rotational relaxation, which does not become effective until after the initial translational motions are complete. This type of delayed onset for rotational motions has been observed in previous simulation studies involving solute size changes⁷ or significant electrostriction.¹⁷ This rotational delay is attributed to the randomization of dipole orientations of the first or second solvent shell or both, as time-dependent orientation distributions have shown.¹⁸ The third, long time, regime, which consists mainly of translations and Lennard-Jones interactions, can be seen clearly in the Lennard-Jones projection in Figure 2b after ~ 450 fs. This long-time relaxation dynamics seen in $S_{\text{LJ}}(t)$, $S_{\text{trans}}(t)$, and $S_{\text{tot}}(t)$ is what would be expected from whole-system repacking on diffusional time scales. A detailed analysis of the motions present at equilibrium and during nonequilibrium dynamics will be presented in forthcoming work.¹⁸

In summary, we have shown that the equilibrium and nonequilibrium dynamics of this system are unrelated, despite the fact that the total response functions in Figure 1 show similar

relaxation time scales. Even though $S(t)$ and $C(t)$ are not rigorously identical,¹¹ they are similar enough that one would not ordinarily anticipate such vast differences in the solute and solvent motions underlying the relaxation dynamics. However, the results in Figures 2 and 4 clearly demonstrate that any similarity between the equilibrium solvation TCF, $C(t)$, and the nonequilibrium solvation response function, $S(t)$, is purely coincidental. This has important implications for both experimental and theoretical studies of solvation dynamics. Equilibrium solvation dynamics are measured in experiments such as transient hole burning,¹⁹ while nonequilibrium solvation dynamics are probed by time-dependent Stokes shift or photon echo spectroscopies.¹ The results presented above show that even if the two experiments give identical results, the underlying molecular motions are not necessarily the same. For simulation studies, it is clear that the mere agreement of $C(t)$ and $S(t)$ is not sufficient to guarantee LR. Instead, a detailed analysis of the molecular motions both at and away from equilibrium must be made to justify the linear response approximation.

Acknowledgment. This work was supported by the National Science Foundation through Grant CHE-0240776. B.J.S. is a Cottrell Scholar of Research Corporation and a Camille Dreyfus Teacher-Scholar. We also thank Erik R. Barthel for his assistance in creating the figures.

Appendix

The results presented in Figures 1–4 were obtained from constant E , V , N molecular dynamics simulations of a charged atomic (Lennard-Jones) solute and 255 THF solvent molecules. The simulations used a 1 fs time step and a modified SHAKE algorithm²⁰ to keep the molecules rigid and planar and employed periodic boundary conditions. The site–site interaction potential was a pairwise sum of Coulomb and Lennard-Jones interactions, using the five-site solvent molecule geometry and potential parameters previously developed by Jorgensen.²¹ We chose the interaction potential parameters for the solute to model the conversion of a solvated sodium anion into a solvated neutral sodium atom to imitate femtosecond experiments studying charge-transfer-to-solvent reactions performed in our lab.²² The excited-state solute (sodium atom) had a Lennard-Jones well depth ($\epsilon = 1.47 \times 10^{-20}$ J) and size ($\sigma = 3.14$ Å) parameter, which were taken from DFT calculations of Rice and co-workers.²³ The ground-state (sodium anion) size parameter ($\sigma = 5.21$ Å) was estimated from the crystal structures obtained by Dye and co-workers,²⁴ and we used polarizability measurements of Edwards and co-workers²⁵ to estimate an energy parameter ($\epsilon = 3.11 \times 10^{-21}$ J). For the solute–solvent Lennard-Jones interactions, we used the standard Lorentz–Berthelot combining rules.²⁶ The ground-state solute contained a charge of $-e$ that interacted by the Coulomb interaction with the partial charges on the oxygen and α -methyls on each THF solvent molecule.

Starting from an fcc-lattice, we equilibrated the systems for 5 ps using a velocity rescaling technique followed by at least 10 ps of additional equilibration. We did not start collecting statistics until we ensured that the solute–solvent system was fully equilibrated by checking that memory of the initial fcc order had fully decayed and that there was no further drift in the average temperature. Once fully equilibrated, we then ran the ground-state equilibrium simulation for 200 ps. We also ran 200 nonequilibrium trajectories by choosing uncorrelated configurations²⁷ from the ground-state equilibrium (sodium anion)

run and instantly removing the charge and changing the Lennard-Jones parameters to those of the excited state (sodium atom) while keeping the velocities unchanged. To mimic a resonant absorption, starting configurations for the nonequilibrium simulations were chosen by requiring the solute-solvent potential energy gap, ΔE , to be within 0.75% of the equilibrium average. Each nonequilibrium trajectory ran for 12 ps. Further details of the equilibrium and nonequilibrium simulations are to be presented in a forthcoming paper.¹⁸

References and Notes

- (1) (a) Maroncelli, M. *J. Mol. Liq.* **1993**, *57*, 1. (b) Cho, M.; Fleming, G. R. *Annu. Rev. Phys. Chem.* **1996**, *47*, 109. (c) Rossky, P. J.; Simon, J. D. *Nature* **1994**, *370*, 263. (d) DeBoeij, W. P.; Pshenichnikov, M. S.; Weirisma, D. A. *Annu. Rev. Phys. Chem.* **1998**, *49*, 99. (e) Stratt, R. M.; Maroncelli, M. *J. Phys. Chem.* **1996**, *100*, 12981.
- (2) Chandler, D. *Introduction to Modern Statistical Mechanics*; Oxford University Press: New York, 1987.
- (3) (a) Maroncelli, M.; Fleming, G. R. *J. Chem. Phys.* **1998**, *89*, 5044. (b) Schwartz, B. J.; Rossky, P. J. *J. Chem. Phys.* **1994**, *101*, 6902. (c) Ladanyi, B. M.; Perng, B.-C. *J. Phys. Chem. A* **2002**, *106*, 6922.
- (4) Munir, S.; Ladanyi, M. *J. Phys. Chem.* **1996**, *100* (46), 18258.
- (5) Day, T. J. F.; Patey, G. N. *J. Chem. Phys.* **1999**, *110*, 10937.
- (6) Laria, D.; Skaf, M. S. *J. Chem. Phys.* **1999**, *111*, 300.
- (7) Aherne, D.; Tran, V.; Schwartz, B. J. *J. Phys. Chem. B* **2000**, *104* (22), 5382.
- (8) (a) Sesé, G.; Padró, J. A. *J. Chem. Phys.* **1998**, *108* (15), 6347. (b) Yamaguchi, T.; Kimura, Y.; Hirota, N. *J. Chem. Phys.* **1999**, *111*, 4169. (c) Chang, S. L.; Wu, T.-M. *Chem. Phys. Lett.* **2000**, *324*, 381. (d) Nishiyama, K.; Hirata, F.; Okada, T. *J. Chem. Phys.* **2003**, *118* (5), 2279.
- (9) Standard deviations for $C(t)$ were calculated by breaking up the 200 ps equilibrium simulation into 126 10 ps blocks with each starting point separated by 1.5 ps. These blocks were correlated as per eq 2 and then averaged.
- (10) The excited-state equilibrium energy gap, $\overline{\Delta E(\infty)}$, is used to normalize $S(t)$. The dashed curve in Figure 1 and the data in Figures 2 and 4 are normalized to the average energy gap between 7 and 12 ps. The dotted curve in Figure 1 is normalized to the average between 2 and 3 ps.
- (11) The response curves in Figure 1 are not identical, but they do possess similar early and long-time features. Despite the small deviations, one might expect the underlying dynamics to be very similar, implying LR.
- (12) Perera, L.; Berkowitz, M. *J. Chem. Phys.* **1992**, *96* (4), 3093.
- (13) Steele, W. A. *Mol. Phys.* **1987**, *61* (4), 1031.
- (14) Ladanyi, B. M.; Maroncelli, M. *J. Chem. Phys.* **1998**, *109* (8), 3204.
- (15) Ladanyi, B. M.; Stratt, R. M. *J. Phys. Chem. A* **1998**, *102*, 1068.
- (16) We have combined the three directions into a single projection, so $B_{\text{trans}}(t)$ refers to the sum of the center of mass translations.
- (17) Rao, M.; Berne, B. J. *J. Phys. Chem.* **1981**, *85*, 1498.
- (18) Bedard-Hearn, M. J.; Larsen, R. E.; Schwartz, B. J., manuscript in preparation.
- (19) See, for example: Ma, J.; Vanden Bout, D. A.; Berg, M. *J. Chem. Phys.* **1995**, *103*, 9146.
- (20) Ciccotti, G.; Ferrario, M.; Ryckaert, J.-P. *Mol. Phys.* **1982**, *47* (6), 1253.
- (21) Chandrasekhar, J.; Jorgensen, W. L. *J. Chem. Phys.* **1982**, *77* (10), 5073.
- (22) (a) Barthel, E. R.; Martini, I. B.; Schwartz, B. *J. Chem. Phys.* **2000**, *112* (21), 9433. (b) Martini, I. B.; Barthel, E. R.; Schwartz, B. *J. Chem. Phys.* **2000**, *113* (24), 11245. (c) Barthel, E. R.; Martini, I. B.; Schwartz, B. *J. Phys. Chem. B* **2001**, *105* (49), 11230. (d) Martini, I. B.; Barthel, E. R.; Schwartz, B. *J. Am. Chem. Soc.* **2002**, *124* (25), 7622.
- (23) Chekmarev, D.; Zhao, M.; Rice, S. A. *J. Chem. Phys.* **1998**, *109* (2), 768.
- (24) Dawes, S. B.; Ward, D. L.; Fussa-Rydel, O.; Huang, R.-H.; Dye, J. L. *Inorg. Chem.* **1989**, *28*, 2.
- (25) Pyper, N. C.; Pike, C. G.; Edwards, P. P. *J. Am. Chem. Soc.* **1993**, *115*, 1468.
- (26) Allen, M. P.; Tildesely, D. J. *Computer Simulation of Liquids*; Oxford University Press: New York, 1987.
- (27) We picked configurations from the ground-state (anion) equilibrium trajectory with an average separation of ~ 1 ps and with a minimum separation of 0.5 ps.